Vol. 5, No. 1, April 2024, page 75-82
JTTM: Jurnal Terapan Teknik Mesin
p ISSN 2721-5377| e ISSN 2721-7825
http://jurnal.sttmcileungsi.ac.id/index.php/jttm

Redesign of venting machine to reduce scrap defect crease in tires manufacture company

Fajar Abdul Aziz*, Subekti Subekti

* Department of Mechanical Engineering, Faculty of Engineering, Mercu Buana University, Jakarta, Indonesia
Jln. Raya Meruya Selatan No.1 West Jakarta, Indonesia

*✉ fajarabdaziz2305@gmail.com

Submitted: 29/10/2023 Revised: 19/11/2023 Accepted: 26/11/2023

Abstract: An apparatus for venting or perforating green tires in order to release trapped air is known as a-venting machine. Productivity will drop in May and July of 2023 as a result of scrap issues brought on by green tire defect creases. The term "defect crease" refers to a flaw in which the operator's manual hand rotation causes silicon to adhere to the side or tread ending of the green tire. Modifications were made with the intention of reducing scrap brought on by defect creases in order to lessen this issue. In order to eliminate the need for the operator to manually rotate the green tire, the roll driver that was initially fixed was replaced with one that can rotate automatically. The scrap defect decrease was 93.15% lower as a result of the modification, going from 73 ppm in the May–July 2023 period to 5 ppm in the September–November 2023 period.

Keywords: Modification; venting machine; punching process; scrap defect crease

1. INTRODUCTION

Green tire perforation or venting are done with a venting machine, which uses a vertically moving venting needle powered by a cylinder [1]. To make sure the green tire does not stick during the curing or cooking process, silicone is sprayed inside the tire prior to the venting process. The operator transfers the green tire to the venting machine so that the venting process can begin after the silicone has been sprayed [2]. To create holes in the sections of the green tire that haven't been subjected to the venting process, the operator must manually rotate the tire. There is a chance that a defect crease will appear if the operator manually rotates the green tire. Defect crease is a flaw that results from the operator manually rotating the green tire by hand, causing silicone to adhere to the side or tread ending [3]. One of the reasons for not meeting the scrap tire target in the GTS section is the high scrap defect crease, which peaked in May–July 2023 at 73 parts per million. The final step in the production of tires is tire maintenance [4]. There are a number of steps that need to be taken when producing tires. The steps involved in creating semi-finished tire materials (green tires), combining raw materials, and curing (cooking green tires into tires that are ready to be marketed) [5]. After being assembled, the environmentally friendly tires are placed in the curing area to be vulcanized [6]. Vulcanization under high pressure and temperature is the curing process [7].

The effectiveness of machine modifications to lower the number of canvas defects has been covered in earlier research [8]. By extending the linner cloth's length, adjusting the motor's tension and torque settings, switching the pressure brake from manual to automatic, raising the linner treatment's pressure brake value, and applying the treatment to the linner by two persons, we were able to successfully overcome the defects in the canvas treatment in this study [9]. Nevertheless, this study does not analyze modified component calculations; rather, it solely addresses the reduction of product defects [10]. At Mercubuana University, numerous design systems have been developed, including the redesign of the motorcycle rocker arm [11], the creation of cutting machines [12], the design of organic fertilizer tablets [13] and simulations on the creation of diabetes-curing robots [14].

A venting machine modification procedure was used to address the aforementioned issues with the goal of lowering scrap defect crease. By converting the fixed roll driver axle into a rotating axle and adding a motor, pillow block, sprocket, and chain as the transmission, along with a rotating or

driving medium. In addition, this modification adds a safety iron for the venting needle, a mount for the motor, and a mount for the pillow block. Because the operator no longer has to manually rotate the green tires, this modification also reduces the possibility of scrap defect creases.

2. METHOD

To get the best results from modifications, it's critical to create a plan before beginning. By swapping out the axle roll driver that was initially fixed for a rotating axle roll driver, the author modifies a portion of the axle roll driver. There are steps in the research process that must be completed in order for this study to be conducted. Figure 1 illustrates how these steps might be shown in a flow diagram.

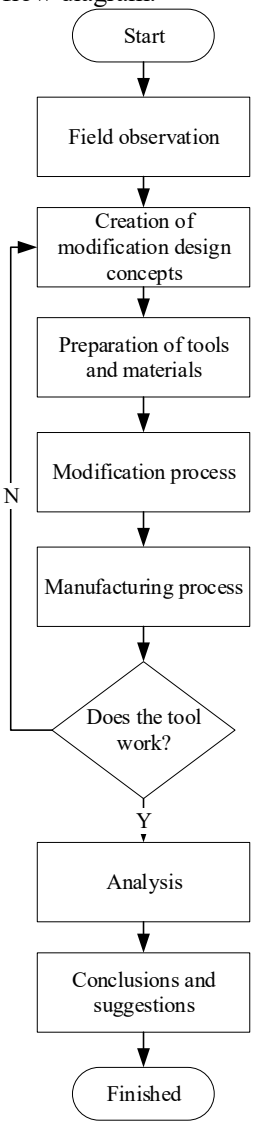

Figure 1. Modification flow diagram

2.1 Data collection stages

The following are the phases of data collection that were completed for this modification:

- Direct research: In direct research, a field study is conducted to ascertain the real conditions in the production process in order to obtain the supporting information required for the assignment's completion. There are various methods for gathering information, including:
  a) Primary data
  Through direct observations of the production process, interviews, and other methods, information about the products produced, the kinds of defects that occur in the product, the

quantity of defects that occur, and the mechanisms underlying the defects can all be obtained. After that, interviews were done to get firsthand knowledge of the kinds of flaws that could have an impact on the quality of the product and to find out what caused the defects to occur.

b) Secondary data
We review company documents, production process data, and the number of defects that have occurred that have been input by the production team in order to gather this data; we do not have direct field experience.

- At this point in the data collection process, a literature study is conducted in the library to gather a number of references from a variety of articles, journals, and theses from research that has been conducted and is, of course, connected to the title that will be covered.

2.2 Machine working system

The machine's functionality remains unchanged from its pre-modification state following the completion of the modification procedure. The driver roll axle makes a difference because it has the ability to rotate automatically, saving the operator from having to manually rotate the green tire. The author added two UCP 206 pillow blocks as bearing media for the axle roll driver in addition to changing the axle roll driver's size to 30 mm. The author then included chains and sprockets as the transmission medium and a three-phase motor as the axle roll driver's driving medium. The author included a safety needle venting iron in the last phase, which allows the user to work securely.

3. RESULTS AND DISCUSSION

3.1 Calculation of weight of modified components

The purpose of this section is to determine each modified component's weight value. in order to make the process of subsequent calculations simpler. To find the volume of each component in this calculation, we apply modified components based on the type of material using Solidworks 2019 software. This ensures that the final weight value is more accurate and in line with field conditions. The weight of each part of the venting engine modification is calculated as follows.

The roll driver in this design has a volume of 4605099.66 mm^3 and employs 1060 alloy material with a density of 2700 kg/m^3, or the equivalent of 0.0027 $gram/mm^3$. Thus, equation (1) can be used to determine the roll driver's mass. (1) [15].

$$m = \rho \times v \quad (1)$$
$$m = 0{,}0027\ gram/mm^3 \times 4605099{,}66\ mm^3$$
$$m = 12433{,}769082\ gram\ =\ 12{,}43\ kg$$

To calculate the load you can use the equation (2) [15].

$$W = m \times g \quad (2)$$
$$W = 12{,}43\ kg \times 9{,}8 m/s^2$$
$$W = 121{,}81\ N$$

This design employs steel alloy material with a volume of 565486.68 mm^3 and a material density of 7700 kg/m^3, or the equivalent of 0.0077 $grams/mm^3$. Thus, equation can be used to determine the axle roll driver's mass (3) [15].

$$m = \rho \times v \quad (3)$$
$$m = 0{,}0077\ gram/mm^3 \times 565486.68\ mm^3$$
$$m = 4354{,}247436\ gram\ =\ 4{,}35\ kg$$

To calculate the load, you can use equation (4) [15]

$$W = m \times g \quad (4)$$
$$W = 4{,}35\ kg \times 9{,}8 m/s^2$$
$$W = 42{,}63\ N$$

Pillow block, the mass of the UCP 210 pillow block is 2700 grams or 2.7 kg, so to calculate the load you can use equation (5) [16].

$$W = m \times g \quad (5)$$
$$W = 2{,}7\ kg \times 9{,}8 m/s^2$$
$$W = 26{,}46\ N$$

With a volume of 33156.81 mm^3, the sprocket in this design is made of cast carbon steel with a density of 7800 kg/m^3, or the equivalent of 0.0078 $gram/mm^3$. Therefore, equation (6) can be used to find the mass of the sprocket [15].

$$m = \rho \times v \quad (6)$$
$$m = 0{,}0078\ gram/mm^3 \times 33156{,}81\ mm^3$$
$$m = 258{,}623118\ gram = 0{,}25\ kg$$

To calculate the load, you can use equation (7) [15].

$$W = m \times g \quad (7)$$
$$W = 0{,}25\ kg \times 9{,}8 m/s^2$$
$$W = 2{,}45\ N$$

Chain, the mass of the chain is 231.66 grams or 0.23 kg, so to calculate the load you can use equation (8) [15].

$$W = m \times g \quad (8)$$
$$W = m \times 9{,}8\ m/s^2$$
$$W = 2{,}25\ N$$

3.2 Analysis of axle driver calculations

When calculating the load on the axle roll driver, the weight of the roll driver plus the green tire constitute the load that the axle roll driver receives. where the W green tire weighs 9.92 kg, or roughly 97.22 N, and the W roll driver is 121.81 N. Thus, the roll driver received a total weight of 121.81 N plus 97.22 N, or 219.03 N.

Equation (9) is used to calculate the bending moment of the axle roll driver since the weight it receives is 219.03 N and the load distance is 350 mm [16].

$$M = W \times L \quad (9)$$
$$M = 219{,}03 \times 350mm$$
$$M = 76660{,}5\ N/mm$$

The axle roll driver is made of alloy steel, which has a tensile strength of 723.8256 N/mm^2. This information is used to calculate the permissible bending stress. Equation (10) is permitted by the bending stress because the safety factor (i) is 8 [16].

$$\sigma b\ izin = \frac{\sigma t}{FS} \quad (10)$$

$$\sigma b\ izin = \frac{723{,}8256\ N/\ mm^2}{8}$$

$$\sigma b\ izin = 90{,}48\ N/\ mm^2$$

Maximum deflection calculation: Use equation (11) to compute the moment of inertia prior to calculating the axle roll driver's maximum deflection [16].

$$I = \frac{\pi d^4}{64} \quad (11)$$

$$I = \frac{3{,}14\ x\ 30^4}{64}$$

$$I = 39740{,}62$$

Equation (12) is used to calculate the maximum deflection following the computation of the moment of inertia. The maximum deflection can be found as follows since the modulus of elasticity of alloy steel is previously known to be 210000 Nmm^2 [16]:

$$\delta = \frac{W.L^3}{3.E.I} \quad (12)$$

$$\delta = \frac{219{,}03 \text{ x } .350^3}{3 \text{ x } 210000 \text{ x } 39740{,}62}$$

$$\delta = \frac{9390911250}{25036590600}$$

δ = 0,38 mm

Meanwhile, the deflection is allowed using equation (13) [16].

$$Y_{izin} = \frac{I}{240} \quad (13)$$

$$Y_{izin} = \frac{350}{240}$$

Y_{izin} = 1,46 mm

Calculations have shown that 1.46 mm is the permissible deflection and 0.38 mm is the maximum that can occur. in order for the roll driver axle to be deemed safe to support the roll driver and green tire load.

The vertical reaction at clamp support A is calculated by applying equation (14) [17].

$$RAV = P \quad (14)$$

RAV = 219,03 N.

Calculation of the reaction moment at clamp support A, reaction moment at support clamp A using equation (15) [17].

$$MA = - (P.L) \quad (15)$$

MA = - (219,03 N x 350 mm)
MA = -76660,5 N/mm

Calculation of shear force, shear force at each point of the cross section using equations (16) and (17) [17].

$$DA = RAV = 219{,}03 \text{ N} \quad (16)$$

$$DB = DA - P = 219{,}03 \text{ N} - 219{,}03 \text{ N} = 0 \text{ N} \quad (17)$$

Figure 2 SFD and BMD images of the cantilever beam.

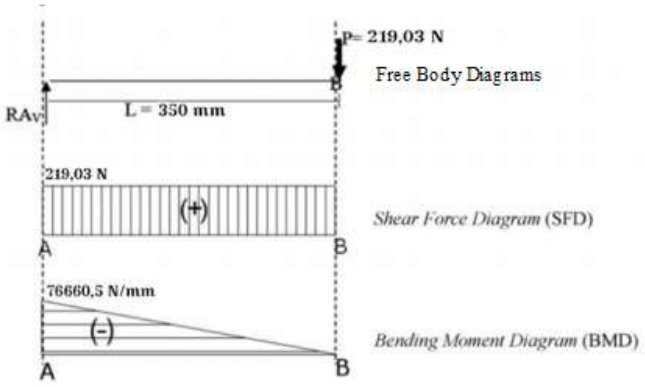

Figure 2. SFD and BMD

3.3 Chain and sprocket planning

Chain and sprocket power plan. Finding the design power of the chain and sprockets can be calculated using equation (18) [15].

$$Pd = Fc \text{ x } P \quad (18)$$

Pd = 1,3 x 0,4 kW

Pd = 0,52 Kw

Chain speed, to find the chain speed using equation (19) [15].

$$V = \frac{P \text{ x } z1 \text{ x } n1}{60 \text{ x } 1000} \quad (19)$$

$$V = \frac{15,87 \text{ x } 13 \text{ x } 37}{60 \text{ x } 1000}$$

$$V = \frac{7633,47}{60000}$$

V = 0,13 m/s

Force on the chain, to find the force on the chain using equation (20) [15].

$$Fg = \frac{102 \text{ x } Pd}{V} \quad (20)$$

$$Fg = \frac{102 \text{ x } 0,52}{0,13}$$

Fg = 408 kg

3.4 Motor calculation

Calculating torque, to calculate the torque that occurs on the shaft, you can use equation (21) [16].

T = W x r
T = 224,51 N x 0,015 m
T = 3,36765 Nm

Calculating motor power, to calculate motor power you can use equation (22) [16].

$$P = \frac{T \text{ x } 2\pi \text{ x } n}{60}$$

$$P = \frac{3,36765 \text{ x } 2(3,14) \text{ x } 1350}{60}$$

P = 475,848945 Watt

P = 0,64 HP

3.5 Condition of the machine after and after modification

In this section, several changes in the condition of the machine before and after modifications are carried out are in Figure 3 and Figure 4.

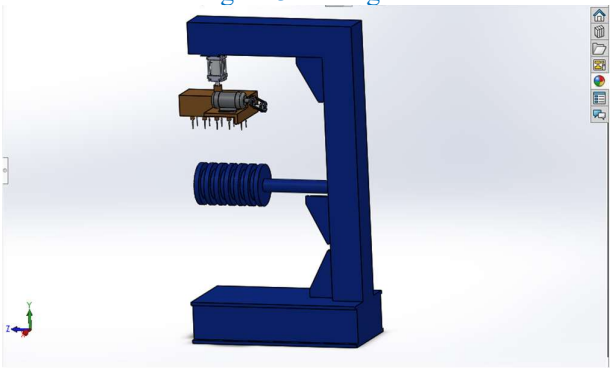

Figure 3. Before modification

Figure 3 the state of the machine in its original configuration. It has an 80mm-diameter roll driver axle with a roll driver attached to its end. Due to its continued fixation and attachment to the venting machine body, the driver roll axle is unable to rotate in this state.

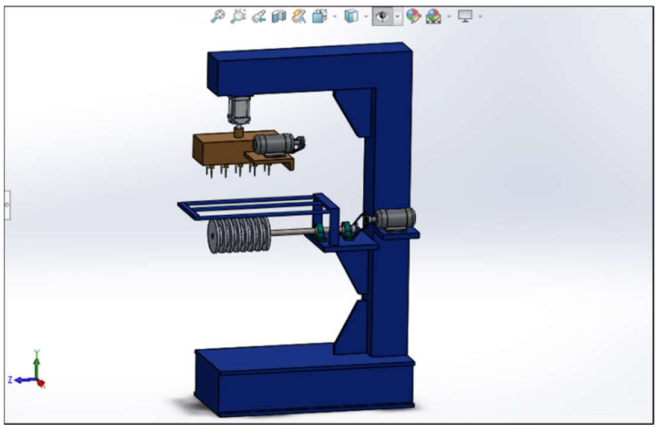

Figure 4. After modification

Figure 4 the machine's condition following modification. It has a roll driver axle with a diameter of 30 mm and a roll driver attached to the end of the axle. Because the roll driver axle is not fixed to the venting machine body and is instead connected to a three-phase motor, it can rotate in this condition.

3.6 Achievement results after modification

From the results of the venting engine modifications that have been carried out, there is comparative data before and after the modification as shown in Figure 5.

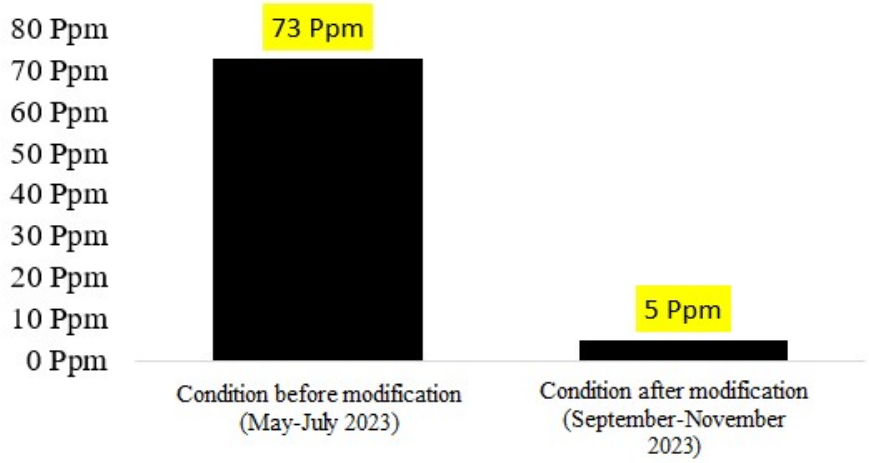

Figure 5. Defect data before and after modification

Figure 5 demonstrates that following modification, there is a notable decrease. Following implementation, the changes proceeded smoothly and in line with the original goal, which was to decrease scrap defect crease. From 73 ppm in the May–July 2023 period to 5 ppm in the September–November 2023 period, there was a 93.15% decrease in scrap defect.

3 CONCLUSION

According to the modification results, the scrap defect crease decreased from 73 ppm in the May–July 2023 period to 5 ppm in the September–November 2023 period, a 93.15% decrease. In order to classify the roll driver axle as safe to support the load of the roll driver and green tire, the axle driver modification results indicate that the maximum deflection that occurred was 0.38 mm, while the permissible deflection is 1.46 mm. Therefore, 0.64 HP of motor power is needed for this modification.

ACKNOWLEDGEMENT

We would like to thank the company PT Gajah Tunggal who has provided facilities to carry out this modification, and do not forget to colleagues from Mercubuana University who have helped in completing this journal.

REFERENCE

[1] M. A. G. Irawan and M. R. A. Cahyono, "Modifikasi Desain Kontruksi Press Tread (Studi Kasus Building Machine Tire Motorcyle)," *Indones. J. Eng. Technol.*, vol. 4, no. 1, pp. 5–14, 2021, doi: 10.26740/inajet.v4n1.p5-14.

[2] A. Syukron, "Modifikasi Sistem Kontrol Mesin Curing Press BTC G17 di PT .Gajah Tunggal TBK," 2009. [Online]. Available: https://repository.mercubuana.ac.id/25429/

[3] H. H. Azwir and A. S. Ratum, "Penurunan Scrap Bead Ban (Blister bead) Di Area Curing Pada Produk Ban Roda Empat Dengan Konsep Siklus PDCA," *J. Ind. Eng.*, vol. 8, no. 1, pp. 46–57, 2023.

[4] M. Marjan, S. Bastuti, and M. Mualif, "Analisis Pengendalian Kualitas Produk Meter Assy Model BBC Menggunakan Metode Six Sigma Untuk Mengurangi Defect Gores di PT Indonesia Nippon Seiki," pp. 186–199, 2022.

[5] R. A. Setiawan and E. Sumarno, "Modifikasi Sistem Kontrol Mesin Curing Guna Mengurangi Defect Leaky Bladder Di Pt Xyz Tbk," *J. Inform. dan Tek. Elektro Terap.*, vol. 11, no. 3, pp. 614–619, 2023, doi: 10.23960/jitet.v11i3.3249.

[6] M. Agustin and M. M. Arifin, "Penerapan Metode DMAIC Untuk Menurunkan Loss Production Material Shortage Pada Proses Curing di Tyre Manufacturing," *J. Kalibr. - Karya Lintas Ilmu Bid. Rekayasa Arsitektur, Sipil, Ind.*, vol. 5, no. 2, pp. 131–137, 2022, doi: 10.37721/kalibrasi.v5i2.1070.

[7] I. A. Firmansyah and S. Afandi, "Ringkasan Sistem Kontrol Otomatis High Pressure Oil Pump Pada Mesin Curing Tire Press Hydraulic," *J. Instrumentasi dan Teknol. Inform.*, vol. 4, no. 2, pp. 102–110, 2023.

[8] P. Low, R. Mesin, and B. Curing, "Desain Ulang Silinder Hidrolik Untuk Mengurangi Kegagalan Pada," vol. 12, no. 1, pp. 46–52.

[9] B. Primanintyo, M. Y. Syafei, and D. Luviyanti, "Analisis Penurunan Jumlah Defect Dalam Proses Tire-Curing Dengan Penerapan Konsep Six Sigma," *J. Ind. Eng.*, vol. 1, no. 2, pp. 1–16, 2016.

[10] Z. Iklima, B. Nur Rohman, R. Muwardi, A. Khan, and Z. Arifiansyah, "Defect classification of radius shaping in the tire curing process using Fine-Tuned Deep Neural Network," *Sinergi*, vol. 26, no. 3, p. 335, 2022, doi: 10.22441/sinergi.2022.3.009.

[11] U. Ls-svm- and A. M. Data, "Fusion Approaches," 2019.

[12] P. A. Nugroho, S. Subekti, and A. Iswahyudi, "Design of organic fertilizer pellet machine with a capacity of 170 . 90 Kg / Hour using verein deutcher ingenieure 2222 method," vol. 4, no. 2, pp. 163–171, 2023.

[13] P. Budi Kurniawan and S. Subekti, "Redesign Cutting Machinemelalui Metode Pendekatan Design for Manufacturing and Assembly (Dfma)," *Poros*, vol. 17, no. 2, pp. 79–88, 2021, doi: 10.24912/poros.v17i2.20018.

[14] M. F. Gulang, Z. D. Haq, H. Alpiyanto, and S. Subekti, "Karakteristik dinamik needle bearing pada camshaft dohc suzuki satria fu150 yang telah di modifikasi, dengan metode bump test," *Tek. J. Sains dan Teknol.*, vol. 16, no. 2, 2020, doi: 10.36055/tjst.v16i2.8461.

[15] R. S. Khurmi and J. K. Gupta, "a Textbook of," *Garden*, no. I, p. 14, 2005.

[16] A. Purna Irawan, "Diktat Elemen Mesin," p. 124 hal, 2014.

[17] V. Koten and D. Hasan, "Penentuan Hubungan Antara Defleksi Lateral dan Radial Poros Baja Pada Berbagai Jenis Tumpuan Secara Teoritik," *J. Ilm. Tek. Mesin Cylind.*, vol. 2, no. 1, pp. 57–63, 2014.